

coupled with the inferior feed material reduced CH<sub>4</sub> emission from plant-D.

The lowest rate of CH<sub>4</sub> emission during a day was observed in the early morning hours at 6.00 am, when the ambient and slurry temperatures were lowest (Figure 2). Emission rates were observed to be highest (12.45 and 9.04 g m<sup>-2</sup>h<sup>-1</sup>) during early afternoon at 2.00 pm. Diurnal variation of CH<sub>4</sub> flux was more pronounced in the slurry pit compared to the exposed area of a plant.

The results of the study revealed that changes in seasonal and diurnal temperature affect CH<sub>4</sub> emission from biogas plants to the atmosphere. Methane emission was maximum around 2 pm during summer months, and decreased to a minimum around 6 am during winter months. Taking into account the exposed surface areas around the floating gas holder in a 85 m<sup>3</sup> biogas plant (1.63 m<sup>2</sup>) and slurry pit (30 m<sup>2</sup>), the annual contribution to global CH<sub>4</sub> budget from a cattle

dung-fed biogas plant, a toilet-linked biogas plant and the slurry pit would amount to 104.6 kg, 50.9 kg, and 667.9 kg respectively.

1. Sarkar, A. N., *J. Sci. Ind. Res.*, 1982, **41**, 279–291.
2. Debnath, G., Ph D thesis, IARI, 1994.
3. Crutzen, P. J., *Nature*, 1984, **350**, 380–381.
4. Topp, E., *Soil Sci. Plant Nutr.*, 1993, **39**, 707–712.
5. Bowden, R. D., Rullo, G., Stevens, G. R. and Steudler, P. A., *J. Environ. Qual.*, 2000, **29**, 268–276.
6. Hutchinson, G. L. and Moiser, A. R., *Soil Sci. Soc. Am. J.*, 1981, **45**, 311–316.
7. Debnath et al., *Climate Change*, 1996, **33**, 97–109.
8. Biogas technology and utilization, FAO Soil Bulletin No. 40, Food and Agricultural Organization, Rome, 1978.

**ACKNOWLEDGEMENTS.** Financial assistance from the Ministry of Non-Conventional Energy Sources, Government of India, New Delhi, is acknowledged for carrying out this

study under a project entitled 'Greenhouse gas emission from exposed areas of biogas plants'.

Received 28 August 2002; revised accepted 31 December 2002

R. S. KHOIYANGBAM\*  
SUSHIL KUMAR  
M. C. JAIN†  
ARUN KUMAR  
VINOD KUMAR

*Division of Environmental Sciences,  
Indian Agricultural Research Institute,  
New Delhi 110 012, India*

*†Present address: School of Engineering  
and Applied Sciences,  
A-41, Usha Bhavan,  
MCIE Mathura Road,  
New Delhi 110 044, India*

*\*For correspondence.*

*e-mail: khoiyangbam@yahoo.co.in*

## Pyrrhotite inclusions in sphalerite

Barton and Bethke<sup>1</sup>, while discussing the nature of chalcopyrite inclusions in sphalerite wondered, '... why we have not observed pyrite blebs of similar origin forming in a Cu-deficient environment...?' In this communication, we report the presence of pyrrhotite blebs in sphalerite from the Rampura–Agucha Zn–Pb sulphide deposit in Rajasthan. The Rampura–Agucha deposit is a sedimentary exhalative type of deposit hosted by graphite–mica–sillimanite schist<sup>2</sup>. The predominant country rocks are granite gneiss and garnet–biotite–sillimanite gneiss with intercalated bands of calc-silicate rock and amphibolite. The mineral assemblages in the country rocks suggest upper-amphibolite facies metamorphism at peak *P–T* conditions of about 6.2 kb and 650°C (Pradeep Kumar, T.B., unpublished; Sharma<sup>3</sup>). The rocks also underwent intense deformation, manifested by the tight mega- and mesoscopic folds<sup>4</sup> and numerous microstructures in the ore and rock sections<sup>5</sup>.

Independent equidimensional beads and chains of ellipsoidal beads of pyrrhotite are found in sphalerite of Ram-

pura–Agucha. This phenomenon is comparable with the chalcopyrite disease in sphalerite<sup>1,6</sup>. The present communication discusses the nature of pyrrhotite beads in sphalerite. Polished ore slabs were studied in reflected plane polarized light and polished thin sections were studied in transmitted plane polarized light.

Sphalerite in Rampura–Agucha is classified into three types: (i) sphalerite in contact with iron-sulphide minerals (pyrite and/or pyrrhotite); (ii) sphalerite not in contact with iron sulphides and, (iii) sphalerite veins.

Only type-2 sphalerite includes blebs of pyrrhotite. Pyrrhotite occurs in two forms: (i) in association with pyrite, sphalerite and galena, and (ii) as inclusions in sphalerite.

These inclusions occur in two forms: (i) equidimensional inclusions within single grains of sphalerite (Figure 1c and d), and (ii) chains of ellipsoidal beads along grain boundaries (Figure 1a, b and d), which, in three dimensions, look like a grain of sphalerite covered with small beads of pyrrhotite. In other words, they

resemble a 'sphalerite cell' carrying numerous small 'parasitic cell' of pyrrhotite on the surface.

Sphalerite has a bluish-grey colour and an average reflectivity percentage of 17.8. No internal reflections were observed. In transmitted light, with increasing Fe content the colour of sphalerite changes from yellow to red and brown, and opacity increases. Pyrrhotite is pinkish-yellow and strongly anisotropic in reflected light, whereas it is opaque in transmitted light. When the polished thin sections were studied, it was found that surrounding each of the pyrrhotite inclusions in sphalerite, there is a yellow-coloured area due to low Fe content, gradually changing to brownish-red colour due to high Fe content away from the inclusion. The chemical composition of the inclusions and sphalerite around these inclusions is given in Table 1. It can be seen from the data that sphalerite is deficient in sulphur ions relative to total Zn and Fe, while pyrrhotite contains excess sulphur. The relative deficiency of sulphur can be either due to vacant anion sites in the

**Table 1.** Chemical composition of sphalerite and included pyrrhotite

Grain no.	Spot <sup>a</sup>	Zn	Fe	S	Fe + Z (n)	x in (Zn, Fe) <sub>1</sub> S <sub>x</sub>
1	Sph/L/3	45.74	6.23	47.28	51.97	0.91
	Sph/L/2	45.39	5.9	48.09	51.29	0.94
	Sph/L/1	33.56	16.54	49.3	50.1	0.98
	Po/L	1.4	47.01	51.49	48.41	1.06
	Po/M	0.98	46.78	52.09	47.76	1.09
	Po/R	6.05	41.82	51.95	47.87	1.09
	Sph/R1	45.8	5.56	47.92	51.36	0.93
	Sph/R/2	45.7	5.79	48.04	51.49	0.93
2	Sph/R/3	45.68	5.86	48.05	51.54	0.93
	Sph/L/3	45.04	6.16	48.09	51.2	0.94
	Sph/L/2	45.19	6.07	48.17	51.26	0.94
	Sph/L/1	45.28	6.02	48.32	51.3	0.94
	Po	1.72	46.67	51.01	48.39	1.05
	Sph/R/1	41.28	10.18	47.92	51.46	0.93
	Sph/R/2	43.8	6.1	49.45	49.9	0.99
3	Sph/R/3	44.92	6.43	48.12	51.35	0.94
	Sph/L/4	44.29	7.23	48.2	51.52	0.94
	Sph/L/3	43.95	6.13	49.61	50.08	0.99
	Sph/L/2	45.27	5.89	48.59	51.16	0.95
	Sph/L/1	45.05	5.77	48.79	50.82	0.96
	Po	1.85	46.79	51.2	48.64	1.05
	Sph/R/1	45.81	5.57	48.01	51.38	0.93
	Sph/R/2	45.74	5.63	47.92	51.37	0.93
4	Sph/R/3	45.52	5.77	48.11	51.29	0.94
	Sph/R/4	45.33	5.86	48.13	51.19	0.94
	Sph/Incl <sup>b</sup>	43.3	7.41	48.38	50.71	0.95
	Sph/Barren <sup>c</sup>	43.87	6.14	49.44	50.01	0.99

<sup>a</sup>Sph, Sphalerite; Po, Pyrrhotite; L, Left-hand side of grain; R, Right-hand side of grain, number proportional to distance from centre of Po. Grain no. 1 is intragranular inclusion and grain nos 2 and 3 are intergranular inclusions.

<sup>b</sup>Average composition of sphalerite with and without pyrrhotite inclusion. <sup>c</sup>Analyses using Energy Dispersive Spectrometer at Department of Earth Sciences, IIT, Bombay.

sphalerite structure and/or due to additional cations in the interstices. The additional sulphur in pyrrhotite is known to be dissolved sulphur in the lattice<sup>7</sup>. Further data show a gradational boundary between sphalerite and pyrrhotite inclusions. This is so in the case of intra-sphalerite blebs as well as inter-sphalerite blebs.

Barton and Bethke<sup>1</sup> attributed the occurrence of blebs and beads of chalcopyrite in sphalerite to replacement. The vein and sea-floor massive sulphide deposits which they studied were formed in the temperature range of 200–400°C, and have not been subjected subsequently to higher temperatures. Bourtnikov *et al.*<sup>6</sup> suggested that the chalcopyrite inclusions are produced by replacement as a result of interaction of sphalerite with solutions that carry both iron and copper.

However, there remain unanswered questions as to why no other associated mineral is replaced and what could be the source of metals in such secondary solutions.

In the present case, had the pyrrhotite beads been exclusively within the sphalerite grains, it is possible that they were cognetic. As most of the beads are sticking to the surface of sphalerite grains, a post-sphalerite process might be responsible for the formation of the beads. This observation led Bourtnikov *et al.*<sup>6</sup> to attribute possibility of solid-state diffusion of Fe through and out of the sphalerite structure and nucleation of pyrrhotite under metamorphic conditions.

On the average, barren sphalerite contains 0.57% Zn and 1.06% S in excess and 1.27% less Fe compared to

sphalerite with pyrrhotite inclusions. This compositional difference may suggest that during metamorphism, iron in sphalerite got re-equilibrated with iron in neighbouring iron-sulphide minerals. Where no iron-sulphide minerals were in contact with sphalerite, it got rid of excess iron, which nucleated to form pyrrhotite.

In most of the metamorphic reactions that take place at elevated *P–T* conditions, mass transfer takes place among the solid phases participating in the reactions. These reactions often lead to the formation of new phases or products as well as transformations within single phases. As transfer of matter in the solid phase is the slowest process in heterogeneous reactions constituting the overall metamorphic process, solid-state diffusion plays a major role. For example, the

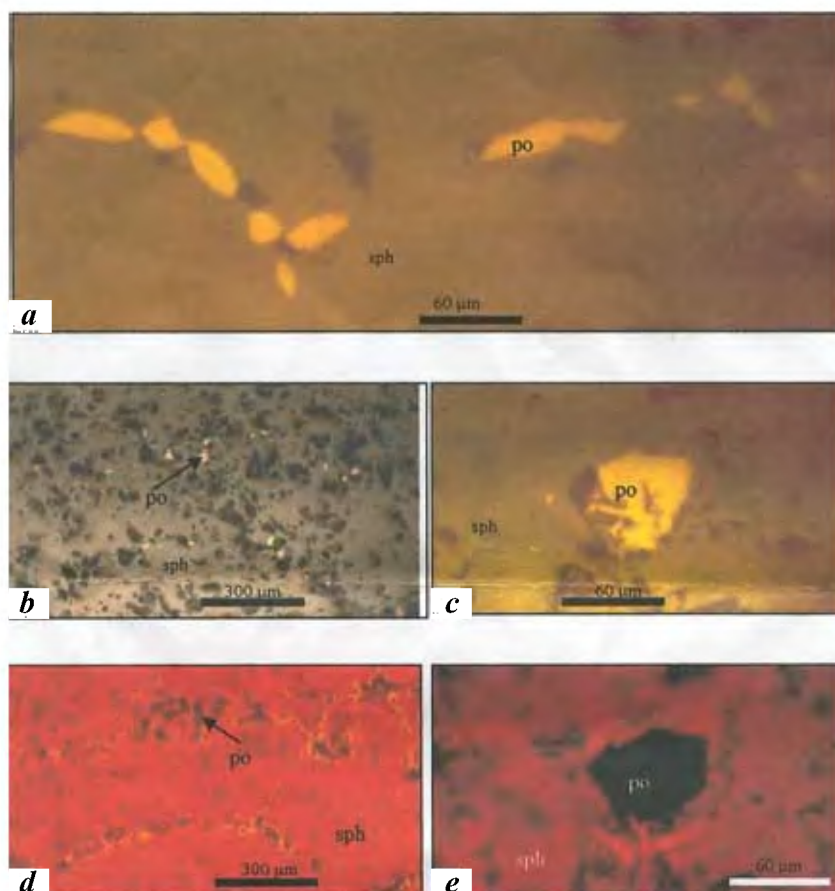


**Figure 1.** Pyrrhotite beads and bead-chains in sphalerite. **a**, Chain of ellipsoidal beads in reflected light; **b**, Bead-chains in reflected light; **c**, Bead-chains in transmitted light. Note the yellow colour of sphalerite around the beads where iron is less; **d**, Single bead in reflected light; **e**, Single bead in transmitted light. Area around the bead is yellow due to less iron content. Po, Pyrrhotite; sph, sphalerite.

rate of oxidation of a metal sulphide mineral during metamorphism is determined by the coefficient of diffusion of the diffusing component. Since polycrystalline material is involved in metamorphism, the theory of diffusion should

describe the transport of matter in the body of the mineral grains as well as along grain boundaries. A factor that governs the possibility of solid-state diffusion as the process of formation of pyrrhotite blebs is the diffusion coeffi-

cient of Fe in sphalerite structure at elevated temperatures of the order of 600°C. Though this process assumes importance, studies in solid-state diffusion mechanisms that operate during metamorphism are few.

1. Barton, P. B. Jr. and Bethke, P. M., *Am. Mineral.*, 1987, **72**, 451–467.
2. Gandhi, S. M., Paliwal, H. V. and Bhatnagar, S. N., *J. Geol. Soc. India*, 1984, **25**, 689–705.
3. Sharma, R. S., *Mem. Geol. Soc. India*, 1988, **7**, 3–31.
4. Ray, J. N., *Indian Miner.*, 1982, **34**, 19–22.
5. Pradeep Kumar, T. B., Jadhav, G. N. and Sahu, B. K., *Mineral Deposits: Processes to Processing* (eds Stanley, et al.), Rotterdam/Brookfield, Balkema, 1999, pp. 771–773.
6. Bourtnikov, N. S., Genkin, A. D., Dobrovolskaya, M. G., Muravitskaya, G. N. and Filimov, A., *Econ. Geol.*, 1991, **86**, 1070–1082.
7. Ramdhor, P., *Ore Minerals and their Intergrowths*, Pergamon, Heidelberg, 1980, 2nd edn.

Received 7 October 2002; revised accepted 4 January 2003

T. B. PRADEEP KUMAR\*<sup>†</sup>  
G. N. JADHAV

*Department of Earth Sciences,  
Indian Institute of Technology,  
Powai,*

*Mumbai 400 076, India*

<sup>†</sup>*Present address: 52/496,  
AMD Flats, Pratap Nagar,  
Jaipur 303 906, India*

*\*For correspondence.*

*e-mail: drpradeepnair@rediffmail.com*